High-Efficiency Planar Antennas for Optoelectronic Phased-Array Communications

(Title Change: Micromachined Micropackaged Microwave and Millimeter-wave Resonators and Low-Loss Filters)

FINAL PROGRESS REPORT

Principal Investigator: Prof. Gabriel M. Rebeiz
Graduate Student: Andrew R. Brown

July 30, 1998

U.S. ARMY RESEARCH OFFICE

Contract: DAAH04-95-1-0205 (ASSERT)
High-Efficiency Planar Antennas for Optoelectronic Phased-Array Communications
Period: July 1995 to July 1998

EECS Department
The University of Michigan
Ann Arbor, MI 48109-2122

33108-1-F = RL-2450

REPORT DOCUMENTATION PAGE

Form Approved
OMB NO. 0704-0188

1. AGENCY USE ONLY (Leave blank)	2. REPORT DATE	3. REPORT TYPE AND DATES COVERED
	7/20/98	FINAL PROGRESS 5/95 - 8/98

4. TITLE AND SUBTITLE
High-Efficiency Planar Antennas for Optoelectronic Phased-Array Communications

5. FUNDING NUMBERS
DAAH04-95-1-0205
P-34276-EL-AAS

6. AUTHOR(S)
Gabriel M. Rebeiz, Andrew R. Brown

7. PERFORMING ORGANIZATION NAME(S) AND ADDRESS(ES)
University of Michigan
1301 Beal Avenue
Ann Arbor, MI 48109-2122

8. PERFORMING ORGANIZATION REPORT NUMBER
033108-1-F

9. SPONSORING / MONITORING AGENCY NAMES(S) AND ADDRESS(ES)
Army Research Office
P.O. Box 12211
Research Triangle Park, NC 27709-2211

10. SPONSORING / MONITORING AGENCY REPORT NUMBER

11. SUPLEMENTARY NOTES
The views, opinions and/or findings contained in this report are those of the author(s) and should not be construed as an official Department of the Army position, policy or decision, unless so designated by other documentation.

12a. DISTRIBUTION / AVAILABILITY STATEMENT
Approved for public release; distribution unlimited.

12b. DISTRIBUTION CODE

13. ABSTRACT (Maximum 200 words)
This report describes the development of novel micromachined micropackaged high-Q resonators and low-loss filters for microwave and millimeter-wave communication systems. The resonators exhibit quality factors of 450-500 at 29,37, and 62 GHz for a microstrip implemetation and 1117 for an 10-12 GHz with greater than 40 dB isolation between elements and 2.3 dB insertion loss. A wideband tunable filter has been developed with a 60% tuning range at 700 MHz to 1.3 GHz with 3 dB insertion size. The tunable filter has been scaled to 10 GHz with a 60% tuning range and 5 dB insertion loss.

14. SUBJECT TERMS
Micromachining, High-Q resonators, Low-loss Filters, Micropackaging, Tunable filters

15. NUMBER IF PAGES
4 plus appendices

16. PRICE CODE

17. SECURITY CLASSIFICATION OR REPORT	18. SECURITY CLASSIFICATION OF THIS PAGE	19. SECURITY CLASSIFICATION OF ABSTRACT	20. LIMITATION OF ABSTRACT
UNCLASSIFIED	UNCLASSIFIED	UNCLASSIFIED	UL

1. Forward

The original contract was based on the development of high-efficiency antennas for optoelectronic phased-arrays. This effort is now well covered at the University of Michigan by an ARO-ASSERT (Thomas Ellis), and by other students (Gildas Gauthier, funded by the Low Power Electronics ARO-MURI and Hughes/DARPA W-band Power Cube Project, and J. D. Schumpert funded also by an ARO-MURI). Therefore, the research of Andrew Brown was shifted to micromachined micropackaged components. This topic is very closely related to the parent ARO contract on micromachining and prepares Andrew well for the 28 GHz micromachined micropackaged digital radio front-end project. The projects, outlined in this report, cover the design and fabrication of high-Q resonators, micropackaged low-loss filter banks, and tunable filters integrated on silicon wafers.

2. List of Appendices

Appendix A - "Micromachined Micropackaged Filter Banks and Tunable Bandpass Filters"

Appendix B - "Micromachined Micropackaged Filter Banks"

Appendix C - "Microwave and Millimeter-wave High-Q Micromachined Resonators"

3. Report Body

A. Statement of the Problem Studied

Alternative techniques for integrating high quality factor resonators using micromachining techniques have been investigated. Conventional resonators suffer from high radiation and ohmic loss. By applying micromachining techniques to alter the geometry of the substrate, high-Q resonators can be realized using standard monolithic fabrication techniques on low cost substrates.

Two types of high performance filters were investigated, interdigitated filter banks and tunable bandpass filters. Both types of filters in conventional form suffer from high cost, multisubstrate design, intricate packaging, and large weight and size [1]. Micromachining and micropackaging were used to allow for a high performance monolithic design on a single low cost substrate with simple conformal packaging [2,3]. This also allows for integration of active elements on the same subtrate as the filters and results in low cost filters in high volume applications.

B. Summary of the Most Important Results

B.1 Millimeter-wave High-Q Resonators.

Two methods were investigated for integrating high-Q resonators. The first method consisted of suspending microstrip lines thin dielectric membranes resulting in an effective dielectric constant of near unity. The second method was by integrating three-dimensional micromachined waveguide cavity resonators with planar feedlines. These resonators show large improvements in quality factor over conventional techniques, and more importantly, allow for planar integration in complex systems. Resonators were fabricated in suspended microstrip at 29, 37, and 62 GHz with quality factors of over 450-500 with very close agreement between simulated and measured results. An integrated micromachined cavity resonator was also fabricated with a TE_{011} resonance quality factor of 1117 at 24 GHz and a TE_{021} resonance quality factor of 1163 at 38 GHz. To the our knowledge, these are the highest quality factor *planar* resonators without the use of superconductive materials, and can be used in microwave and millimeter-wave low-loss filters and low phase noise oscillators (see reprint 3 attached to the report)

B.2 Micromachined Micropackaged Filter Banks

A micromachined filter bank was fabricated on silicon consisting of two interdigitated filters at X/Ku-band. The filters are integrated on thin dielectric membranes which result in low loss. The measured port-to-port insertion loss is 2.3 dB for each filter. The micropackaging provides high isolation between adjacent filters in the overlapping frequency region. The measured isolation between filters was about -40 dB across the passbands of the filters (See reprint 1 attached to the report). This technology allows for the low-cost integration of switched filter banks used predominantly in satellite communication systems and wideband radar.

B.3 Micromachined Tunable Filters and Measurements

A microwave model at 1.25 GHz of the integrated tunable filter was was fabricated. The measured response of the filter showed a 60% tuning bandwidth from 700 MHz to 1.33 GHz. At center frequencies below 1 GHz, the bandwidth is reduced and the insertion loss increases. We believe this is due to the limited bandwidth of the input fingers of the filter. For center frequencies above 1 GHz, the insertion loss is less than 3 dB in the passband. The microwave model alone is comparable to state-of-the-art YIG and mechanically tuned filters at only a fraction of the material and assembly cost [4].

An integrated tunable filter was fabricated at 10 GHz. This is based on the microwave model,

and scaled by a factor of 8. The integrated filter had a 60% tuning range from 5.5 GHz to 10.5 GHz with an insertion loss of 5 dB (See reprint 1 of appendix).

C. List of All Publications and Technical Reports Published

1. A. R. Brown and G. M. Rebeiz, "Micromachined Micropackaged Filter Banks and Tunable Bandpass Filters," *1997 Wireless Communications Conference Digest,* pp. 193-197, Aug. 1997.

2. A. R. Brown and G. M. Rebeiz, "Micromachined Micropackaged Filter Banks," *IEEE Microwave and Guided Wave Letters,* vol. 8, no. 4, April 1998.

3. A. R. Brown, P. Blondy, and G. M. Rebeiz, "Microwave and Millimeter-wave High-Q Micromachined Resonators," *Submitted for review to the International Journal of RF and Microwave Computer-Aided Engineering,* June 1998.

D. List of Participating Scientific Personnel and Advanced Degrees Earned

Andrew R. Brown, Graduate Student, University of Michigan, Degree: Earned Masters of Science in Electrical Engineering in December 1996. Will earn PhD. in May 1999.

Gabriel M. Rebeiz, Professor of Electrical Engineering and Computer Science, University of Michigan.

4. Report of Inventions

"3-Dimensional Integrated Micromachined Cavity Resonator with Planar Feed Structure"

No patent application was filed.

5. Bibliography

[1] G. L. Matthaei, L. Young and E. M. T. Jones, *Microwave Filters, Impedance-Matching Networks, and Coupling Structures.*, chaper 10, pp. 614-650, Artech House, Inc., 1980.

[2] C. Y. Chi and G. M. Rebeiz, "Conductor-Loss Limited Stripline Resonators and Filters," *IEEE trans. Microwave Theory Tech.*, vol. MTT-44, pp. 626-630.

[3] R. F. Drayton, R. M. Henderson, and L. P. B. Katehi, "Advanced monolithic packaging concepts for high performance circuits and antennas", *IEEE MTT-S Int. Microwave Symp. Digest*, pp. 1615-1618, May 1996.

[4] Y. Ishikawa, T. Nishikawa, T. Okada, S. Shinmura, Y. Kamado, F. Kanaya and K. Wakino, "Mechanically tunable MSW bandpass filter with combined magnetic units," *IEEE MTT-S Int. Symp. Digest*, pp. 143-146, May 1990.

Micromachined Micropackaged Filter Banks and Tunable Bandpass Filters

Andrew R. Brown and Gabriel M. Rebeiz
The University of Michigan
1301 Beal Avenue
Ann Arbor, MI 48109
Phone: (313) 936-0183
mscout@engin.umich.edu, rebeiz@engin.umich.edu

Abstract

Low cost alternatives to conventional switched filter banks and tunable bandpass filters are investigated. Both types of filters in conventional form suffer from high cost, intricate packaging, and large weight and size. Micromachining and micropackaging were used to allow for a high performance, monolithic design on a single low cost substrate with simple conformal packaging. A micromachined micropackaged filter bank at X/Ku-band is presented. The filters are fabricated on thin dielectric membranes on silicon wafers allowing for low-loss filters on inexpensive substrates. The micropackaging provides high isolation between adjacent filters with overlapping frequency regions. Also, a novel micromachined electronically tunable filter at X-band is presented. The filter is simple to fabricate and results in a very wide tuning range with low insertion loss. An 8× microwave model was built at 1 GHz to simulate the X-band filter, and an 8 GHz filter was fabricated based on the microwave model. The filter exhibited a tuning range of over 60% for a 10% bandwidth.

Keywords: Filters, Micromachining, Packaging techniques.

I. Introduction

LOW -loss filters are a necessary component in communication systems. Conventional designs for low loss filter banks and tunable filters are not compatible with the goals of industry for low cost materials and assembly, and reduced size and weight.

For the case of filter banks, the conventional design is to machine a series of channels in a metal carrier and to place individual filters inside these channels. An input and output switching network of PIN diodes selects the filter response. Each filter is on a different low-loss substrate and the PIN diodes are placed in a hybrid fashion on the metal carrier (figure 1). The conventional design technique suffers from many drawbacks. The machined metal carrier and packaging is custom made and therefore is very expensive to produce. Furthermore, the use of separate low-loss substrates for filters combined with active semiconductor substrates for PIN diodes is expensive in material and assembly.

Microwave tunable filters are typically mechanically tuned by adjusting the cavity dimensions of the resonators or magnetically altering the resonant frequency of a ferromagnetic yttrium-iron-garnet element [1,2]. Neither of these approaches is compatible with the need for miniaturization and mass produce-ability. The filters must be custom machined, carefully assembled, tuned, and calibrated. For high frequencies, where the resonators are very small, conventional machining is not an option, and mechanical tuning is also a major problem.

This paper shows how silicon micromachining and micropackaging can be applied to filter design to construct low loss filter banks and tunable filters that are a fraction of the cost of conventional approaches, that can be integrated directly with receiver components, and are much smaller and lighter than conventional filters.

Silicon micromachining has been used to fabricate low-loss lumped elements, filters, power dividers, and couplers [3-6]. Monolithic micropackaging by micromachining techniques has also been shown to provide high isolation between planar transmission lines while still being compact and relatively simple to fabricate [7]. It provides light weight and compact size without greatly changing design methodology or requiring multisubtrate designs. This paper demonstrates the capability of

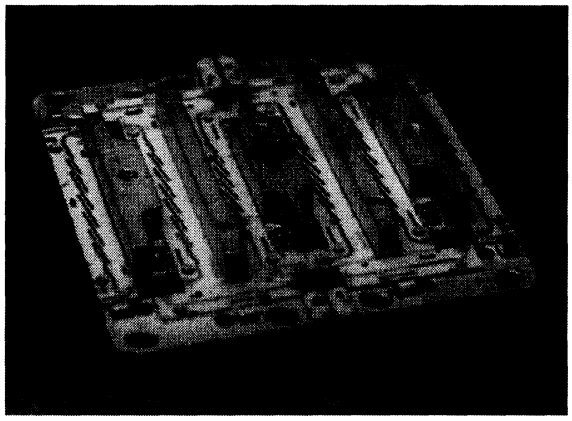

Figure 1. Switched filter bank (*Courtesy of Texas Instruments*).

combining the low-loss characteristic obtained using silicon micromachining and the flexibility and high isolation of micropackaging.

II. Micromachined Filter Banks

A. Design

The micropackage is a two layer structure placed on a bottom carrier substrate. The two layers consist of a micromachined filter substrate and a top cavity substrate (figure 2). The filter substrate layer is a 525 μm silicon membrane wafer. The membrane is a stress compensated tri-layer of silicon dioxide, silicon nitride, and silicon dioxide with a thickness 1.4 μm and a relative dielectric constant of about 7. Surrounding the filters are etched via grooves which prevent substrate modes from forming and most importantly, isolate the two filters. The substrate layer includes the membranes, all metal feedlines, filters, and air bridges. For future designs, this layer could also include active circuits such as PIN diode switches, RF amplifiers, and IF system circuitry using either flip chip technology or device integration.

The cavity substrate is a micromachined wafer that surrounds the filters except for small mouseholes for feedlines to the filters. The cavity is coated with metal (Ti/Al/Ti/Au) approximately 2 μm thick. This isolates the two filters and feed lines from each other. The cavity wafer can easily be designed to accommodate the flip chip PIN diode switches used in the filter bank. For large productions, the cavity substrate could be fabricated using temperature stable plastics.

Alignment marks are placed on the substrate wafer to aid in the assembly of the cavity. The layers are secured to each other with a silver conductive epoxy. The package forms a rugged, compact, and light weight structure.

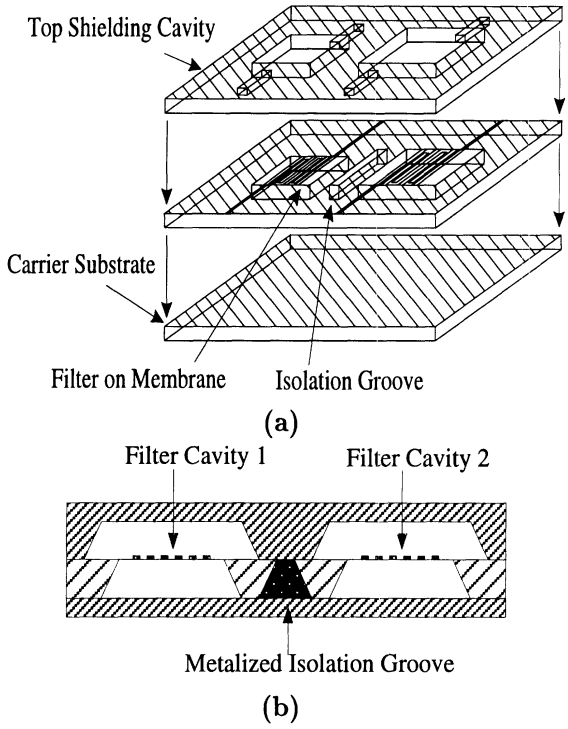

Figure 2. Micropackaging of micromachined filter bank, (a) isometric view, (b) cross section view.

Micromachined interdigitated filters on thin dielectric membranes have been demonstrated by Chi, et al. [5]. The filters were designed based on the procedure developed by Matthaei [2]. The ends of the open stubs of the filters were shortened to take into account added capacitance at the open end of the transmission line. The filters were designed with a 10-12 GHz and a 12-14.5 GHz passband (18% bandwidth). The design procedure did not take into coupling between non-adjacent resonators or the effects of the cavity itself. The feed for the filters is a shielded grounded coplanar waveguide (GCPW) line.

The total surface area of the filter bank is 22.5 mm $\times$ 10.3 mm (figure 3). The entire structure is only 1 mm thick which is about 5$\times$ smaller than conventional switched filter banks.

B. Measurements

The filter response and isolation were measured from 2-16 GHz using a Hewlett Packard 8510C Network analyzer. A Short-Open-Load-Through calibration method was used with 150 μm pitch Picoprobes and a calibration substrate from GGB Industries. The center frequency of the two filters was shifted down by 10%. This may be due to an underestimation in the amount of length to

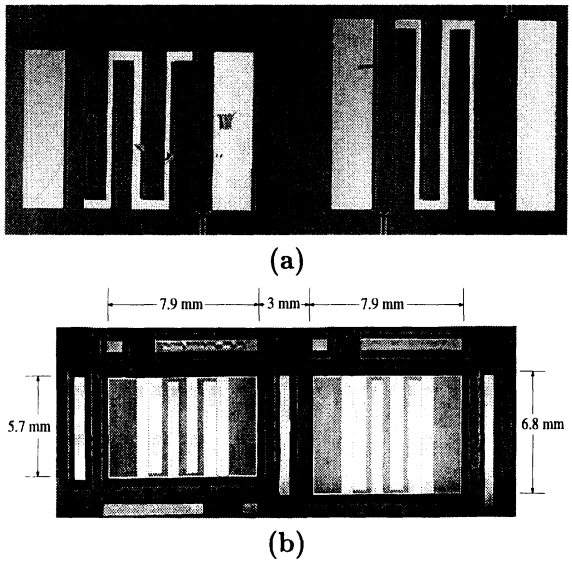

Figure 3. Top view (a) and bottom view (b) of the fabricated micromachined filter bank.

shorten in each resonator. The measured port-to-port insertion loss is 2.3 dB for each filter (figure 4a). The loss of each of the GCPW feed lines is 0.4 dB making a total feedline loss of 0.8 dB (this loss is not removed from the 2.3 dB insertion loss since it is part of the packaging of the system).

The isolation between the filters was measured by loading one filter with a broadband matched load at one port, applying a signal to the other port, and measuring the transmission at the closest port to the other filter. This is the case of the strongest coupling between the two filters. The measured isolation was about -40 dB across the passbands of the filters (figure b). We believe that this is limited by feedline radiation into the 525 μm silicon substrate [7].

III. Tunable Micromachined Bandpass Filters

A. Design

The design of a varactor-loaded interdigitated filter is similar to the capacitively loaded comb-line filter presented in Matthaei [2]. The interdigitated filter is a symmetric filter of coupled resonators. The first finger at the input and output port is a shorted line that acts as an impedance transformer for the filter. This is the only line with a fixed termination. The interior coupled lines are shorted at one end and loaded with varactor diodes at the other end. The width and separation of the interior lines are determined only by the bandwidth of the normalized filter response function, and is independent of the center frequency. The center frequency of the filter is determined by the resonant lengths of the lines which is tuned by the varactors. The limiting factor for the tuneability is the input and output fingers of the filter and the range of capacitance of the varactor diodes until the electrical length of the fingers reaches $\lambda/4$. The center frequency, f_0, can be found by:

$$f_0 \approx \frac{1}{Z_{int} 2\pi C \tan\theta}$$

where Z_{int} is the internal impedance of the filter, C is the junction capacitance of the varactor diode, and θ is the electrical length of the fingers at

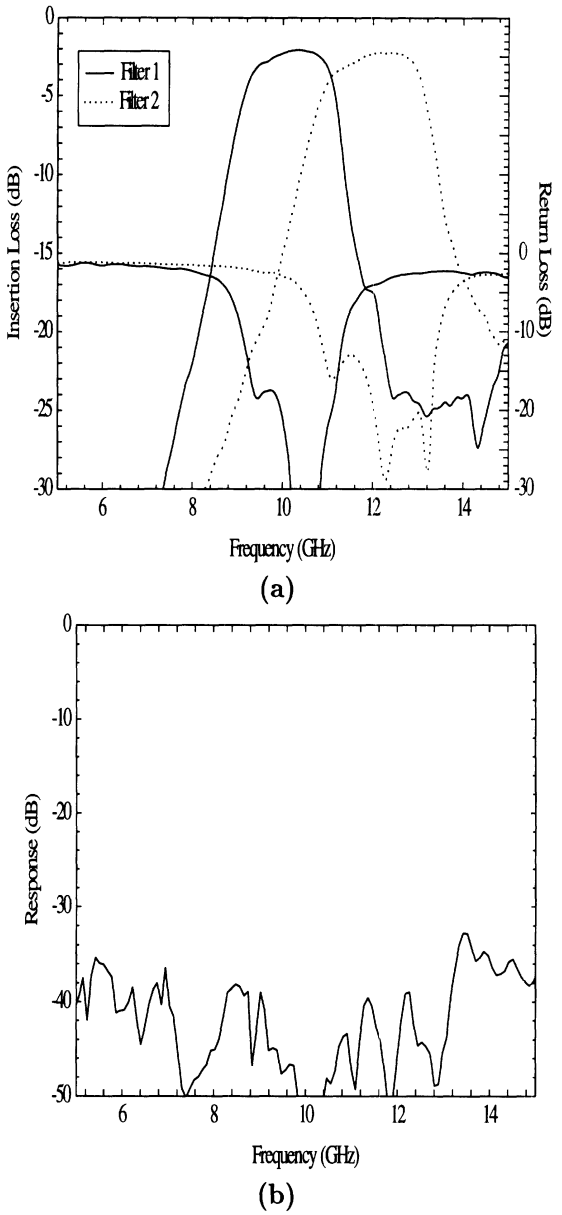

Figure 4. Measured response (a) and isolation (b) of the micropackaged filter bank.

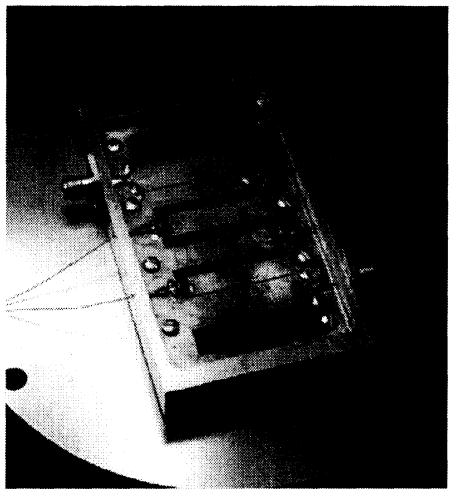

Figure 5. The 1.6 GHz model of a varactor tuned micromachined filter.

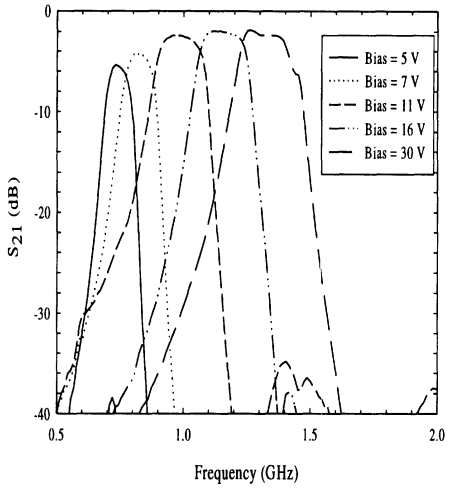

Figure 6. Measured response of the 1.6 GHz model filter for various bias levels.

f_0. For large variation of f_0 with small changes in C, Z_{int} and θ should be small. However, θ should not be so small that the physical dimensions of the varactors become significant compared to the finger length.

The design process used for the tunable interdigitated filter did not take into account the coupling between non-adjacent elements or cavity effects of the filter. To analyze the filter before integration, an 8 × larger microwave model was constructed. The factor of eight was chosen to coincide with the geometry and capacitance scaling of available varactors. Due to the pure TEM mode of the micromachined structure, the model can yield an accurate simulation of the tuned integrated filter.

The model filter was fabricated on 127 μm RT/Duroid with a dielectric constant of 2.2 to simulate the thin dielectric membrane. The finger length is 0.13λ at 1.25 GHz with an internal impedance of 60 Ω and a bandwidth of 10%. The filter was fitted within an aluminum cavity that was milled so as to simulate the micromachined cavity. The varactors are Phillips BB811 UHF Variable Capacitance Diodes with a series resistance of 1.45 Ω and a junction capacitance from 1 pF to 8.8 pF over a 30 V bias range. The varactors are biased in parallel with a 75 pF capacitor which provides an RF short. The predicted tuning range was from 660 MHz to 1.6 GHz (83% tuning range) with all varactors biased equally in parallel (figure 5).

The measured response of the filter showed a 60% tuning bandwidth from 700 MHz to 1.33 GHz (figure 6). At center frequencies below 1 GHz, the bandwidth is reduced and the insertion loss increases. We believe this is due to the limited bandwidth of the input fingers of the filter. For center frequencies above 1 GHz, the insertion loss is less than 3 dB in the passband. The microwave model alone is comparable to state-of-the-art YIG and mechanically tuned filters at only a fraction of the material and assembly cost.

A micromachined tunable filter was fabricated on silicon in a similar manner as with the filter bank. The varactors were biased by breaking the ground plane with a thin slit. Capacitors shorted the slit at the RF frequency preventing any slotline mode propagation. Polyimide used to coat the membrane to prevent the top cavity from shorting out the biasing. The varactors used were M/A Com MA46580 beam lead varactors with capacitance values of 0.1 pF to 1.1 pF for an 18 V Tuning range with a series resistance of 3.5 Ω. The predicted tuning range is from 5.3 GHz to 12.8 GHz. The total area of the filter is 12.1 mm × 7.5 mm × 1 mm which is considerably smaller than a YIG-filter of similar specifications.

B. Measurements

The tunable filters were measured using the same method as with the filter banks above. The varactors were measured to have a capacitance variation of 1.8 pF to 0.18 pF. The measured tuning range was approximately from 5.5 GHz to 10.5 GHz with an insertion loss of about 5 dB (figure 9). The tuning range was limited by varactor capacitance not tuning below 0.18 pF. The insertion loss and the out of band rejection were also degraded. This is due to the upper cavity not having direct contact with the ground and the ground plane being split (necessary to bias the varactors in our de-

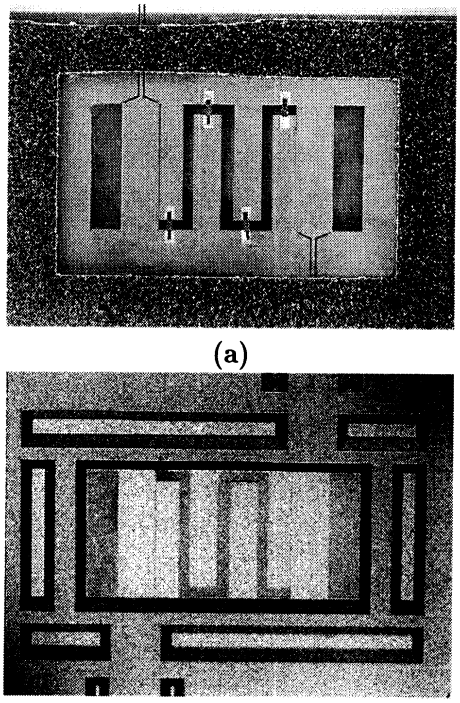

Figure 8. (a) Partially assembled tunable microwave filter, (b) backside of tunable filter.

sign). In future designs, MMIC capacitors should be used for biasing the varactors allowing for better grounding of the top and bottom ground planes of the stripline structure.

IV. Conclusions

This paper demonstrates the capability of combining micromachining and micropackaging techniques to fabricate high performance filter banks and tunable bandpass filters. The processing used is compatible with via-hole fabrication in silicon, SiGe, GaAs, and InP. The cost and size of the filters have serious advantages over conventional design methods.

Acknowledgments

This work is supported by the Army Research Office. The authors would like to thank Dr. Chen-Yu Chi, formerly of the University of Michigan for insight into this project. We would also like to thank Phillips Semiconductor for the donation of varactors and Rogers for donation of RT/Duroid substrates used in the microwave model.

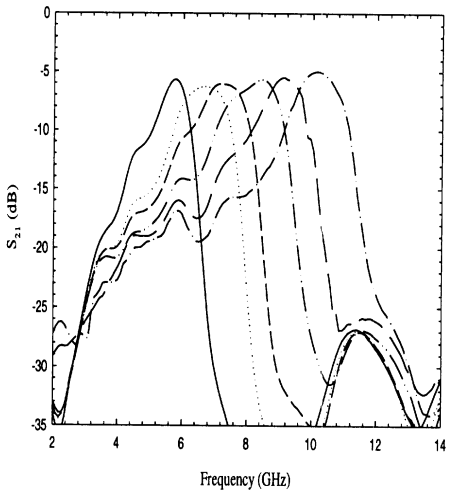

Figure 9. Measured Response of tunable filter.

References

[1] Y. Ishikawa, T. Nishikawa, T. Okada, S. Shinmura, Y. Kamado, F. Kanaya and K. Wakino, "Mechanically tunable MSW bandpass filter with combined magnetic units," *IEEE MTT-S Int. Symp. Digest*, pp. 143-146, May 1990.

[2] G. L. Matthaei, L. Young, and E. M. T. Jones, *Microwave Filters, Impedance-Matching Networks, and Coupling Structures.*, Artech House, Inc., 1980.

[3] C. Y. Chi and G. M. Rebeiz, "Planar microwave and millimeterwave lumped elements and coupled-line filters using micromachining techniques," *IEEE Trans. Microwave Theory Tech.*, vol. MTT-43, pp. 730-738, April 1995.

[4] S. V. Robertson, L. P. Katehi, and G. M. Rebeiz, "Micromachined self-packaged W-band bandpass filters," *1995 IEEE MTT-S Int. Microwave Symp. Digest*, pp. 1543-1546, May 1995.

[5] C. Y. Chi and G. M. Rebeiz, "Conductor-Loss Limited Stripline Resonators and Filter," *IEEE Trans. Microwave Theory Tech.*, vol. MTT-44, pp.626-630.

[6] T. M. Weller, et al., "Membrane technology applied to microstrip: a 33 GHz Wilkenson power divider," *1994 IEEE MTT-S Int. Microwave Symp. Digest*, pp. 911-914, May 1994.

[7] R. F. Drayton, R. M. Henderson, and L. P. Katehi, "Advanced monolithic packaging concepts for high performance circuits and antennas," *1996 IEEE MTT-S Int. Microwave Symp. Digest*, pp. 1615-1618, May 1996.

Micromachined Micropackaged Filter Banks

Andrew R. Brown, *Student Member, IEEE*, and Gabriel M. Rebeiz, *Fellow, IEEE*

Abstract— **A micromachined, micropackaged filter bank at X/Ku-band is presented. The filters are integrated on a silicon substrate, and the micropackaging provides high isolation between the adjacent filters in the overlapping frequency region. This technology allows for the low-cost integration of switched filter banks *on the same substrate* for satellite communication systems, base-stations, and wide-band radar applications.**

Index Terms—**Filters, micromachining, packaging techniques.**

I. Introduction

SWITCHED filter banks are commonly used for multiband communication systems and frequency hopping radar systems where high isolation between the filter elements is a requirement. Also, compact size, reduced weight, and low material and fabrication costs are essential. The conventional design for a switched filter bank is to machine a series of channels in a metal carrier and to place individual filters inside these channels. An input and output switching network of p-i-n diodes selects the filter response (Fig. 1). The conventional design technique suffers from many drawbacks. The machined metal carrier and packaging is custom made and therefore is very expensive to produce. Furthermore, the use of separate low-loss substrates for filters combined with active semiconductor substrates for p-i-n diodes is expensive to assemble. We feel that micromachining, combined with micropackaging, is a possible solution to the cost problem.

Silicon micromachining has been used to fabricate low-loss lumped elements, filters, power dividers, and couplers [1], [2]. Monolithic micropackaging by micromachining techniques has also recently been shown to provide high isolation between planar transmission lines while still being compact and relatively simple to fabricate [3].

The purpose of this work is to demonstrate the capability of combining the low-loss characteristic obtained using membrane technology with the high isolation and compact size obtained using micropackaging. The goal is to construct a high performance X/Ku-band filter bank with high isolation between the filters.

II. Design of Micromachined Filter Banks

The micropackage is a two layer structure placed on a bottom carrier substrate. The two layers consist of a micromachined filter substrate and a top cavity substrate (Fig. 2). The filter substrate layer is a 525-μm silicon membrane wafer. The membrane is a stress compensated tri-layer of SiO_2–Si_3N_4–SiO_2 with a thickness 1.4 μm and a relative dielectric constant of about 7. Surrounding the filters are etched via grooves which prevent substrate modes from forming and most importantly, isolate the two filters. The micromachined filter substrate includes the membranes, all metal feedlines, filters, and air bridges. For future designs, this layer could also include active circuits such as p-i-n diode switches, radio frequency (RF) amplifiers, and intermediate frequency (IF) system circuitry using either flip chip technology or device integration.

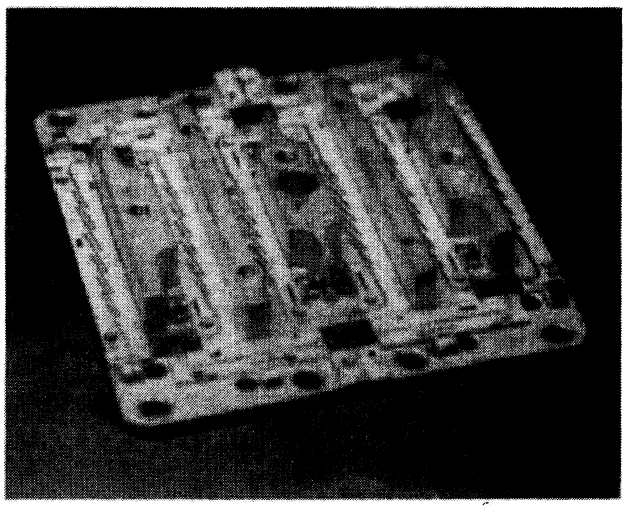

Fig. 1. Switched filter bank (courtesy of Texas Instruments).

The top cavity substrate is a micromachined wafer that surrounds the filters except for small mouse-holes for feedlines to the filters. The cavity is coated with metal (Ti–Al–Ti–Au) approximately 2 μm thick. This isolates the two filters and feed lines from each other. Alignment marks are placed on the micromachined substrate wafer to aid in the assembly of the top cavity wafer. The layers are secured to each other with a silver conductive epoxy. The package forms a rugged, compact, and lightweight structure.

The micromachined filters are based on an interdigital design shown by Matthaei *et al.* [4] and demonstrated recently by Chi *et al.* by using micromachining techniques [2]. However, the micropackaging technique applies to any shielded microstrip or stripline filter design. The feedlines for the filters are 2.4-mm-long shielded grounded coplanar waveguide lines on high-resistivity silicon (ρ = 1200 Ω-cm). The lines extend beyond the via holes of the filter and are not isolated from each other in any other way [Fig. 3(a)]. An airbridge was fabricated

Manuscript received November 3, 1997. This work was supported U.S. Army Research Office under Contract DAAH04-95-1-0205.

The authors are with the Radiation Laboratory, Department of Electrical Engineering, University of Michigan, Ann Arbor, MI 48109 USA (e-mail: mscout@engin.umich.edu; rebeiz@engin.umich.edu).

Publisher Item Identifier S 1051-8207(98)02716-0.

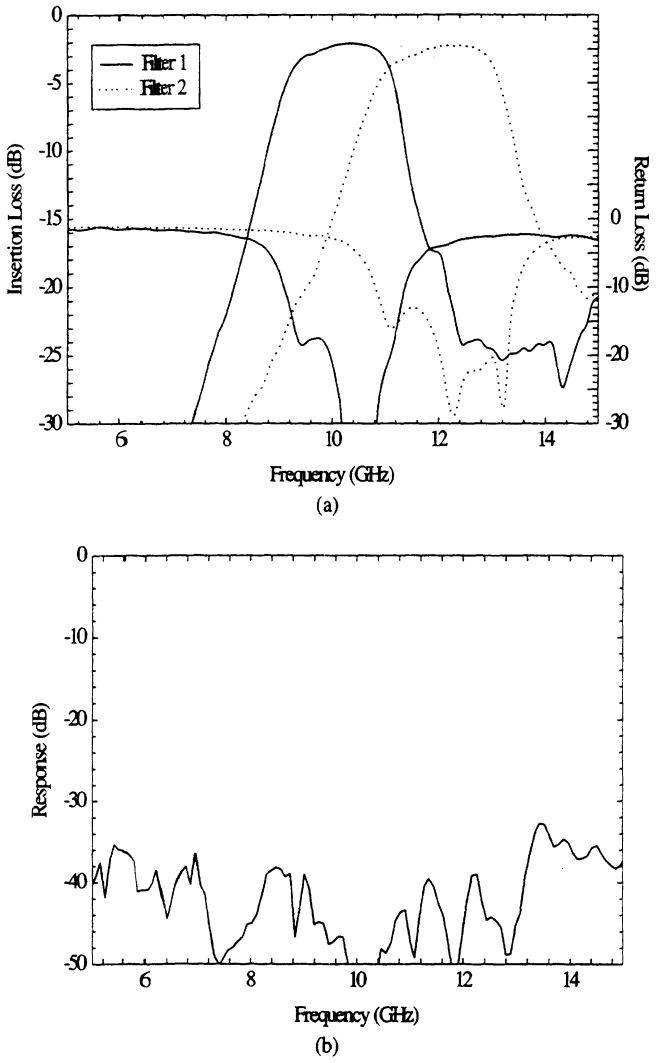

Fig. 4. (a) Measured response and (b) isolation of the micropackaged filter bank.

The measured port-to-port insertion loss is 2 dB for each filter [Fig. 4(a)]. The port-to-port loss includes the feedline loss, the transition loss between the silicon and the membrane, and the loss within the filter. The loss of each of the 0.4 mm GCPW feed lines is 0.4 dB each making a total feedline loss of 0.8 dB. The filter mismatch loss $(1-|S_{11}|^2)$ is 0.4 dB. The theoretical Q of the quarter-wave resonators is 310 using the attenuation coefficient from Zeland Software IE3D. [5]. This results in a calculated loss from the resonator fingers of 0.8 dB [4], and a port-to-port calculated loss of 2 dB, which is in very close agreement with the measurements.

The isolation between the filters was measured by loading one filter with a broad-band matched load at one port, applying a signal to the other port, and measuring the transmission at the closest port to the other filter. This is the case of the strongest coupling between the two filters. The measured isolation was below −40 dB across the passbands of the filters (Fig. 4b). We believe that this is limited by feedline radiation into the 525-μm silicon substrate [3]. It is important to note that micropackaging technologies will never achieve the isolation level obtained using two physically isolated substrates, but it does offer excellent performance for filters integrated close together on the *same* substrate.

IV. Conclusion

This letter demonstrates the capability of combining micromachining and micropackaging techniques to fabricate completely integrated high-performance filter banks with high isolation between elements. The processing used is compatible with via-hole fabrication in Silicon, SiGe, GaAs, and InP. This can result in low cost integration of high performance filter banks for communication systems.

V. Acknowledgments

The authors would like to thank Dr. C.-Y. Chi at Hewlett Packard, Santa Rosa, CA, for discussions and ideas of combining micromachining to microwave circuits.

References

[1] S. V. Robertson, L. P. Katehi, and G. M. Rebeiz, "Micromachined W-band filters," *IEEE Trans. Microwave Theory Tech.*, vol. 44, pp. 598–606.
[2] C. Y. Chi and G. M. Rebeiz, "Conductor-loss limited stripline resonators and filters," *IEEE Trans. Microwave Theory Tech.*, vol. 44, pp. 626–630.
[3] R. F. Drayton, R. M. Henderson, and L. P. Katehi, "Advanced monolithic packaging concepts for high performance circuits and antennas," in *1996 IEEE MTT-S Int. Microwave Symp. Dig.*, May 1996, pp. 1615–1618.
[4] G. L. Matthaei, L. Young, and E. M. T. Jones, *Microwave Filters, Impedance-Matching Networks, and Coupling Structures.* Dedham, MA: Artech House, 1980.
[5] Zeland IE3D Release 4.12, 1997.

Microwave and Millimeter-wave High-Q Micromachined Resonators

Andrew R. Brown, Pierre Blondy, and Gabriel M. Rebeiz

Abstract

Alternative techniques for integrating high quality factor resonators using micromachining techniques have been investigated. Two methods are presented which include suspending microstrip lines thin dielectric membranes resulting in an effective dielectric constant of near unity, and integrating three-dimensional micromachined waveguide cavity resonators with planar feedlines. These resonators show large improvements in quality factor over conventional techniques, and more importantly, allow for planar integration in complex systems. Resonators were fabricated in suspended microstrip at 29, 37, and 62 GHz with quality factors of over 450 with very close agreement between simulated and measured results. An integrated micromachined cavity resonator was also fabricated with a TE_{011} resonance quality factor of 1117 at 24 GHz and a TE_{021} resonance quality factor of 1163 at 38 GHz. To the authors' knowledge, these are the highest quality factor *planar* resonators without the use of superconductive materials, and can be used in microwave and millimeter-wave low-loss filters and low phase noise oscillators.

Keywords

Millimeter-wave, High-Q Resonators, Micromachining, Packaging techniques

I. INTRODUCTION

Microwave and millimeter-wave communication systems are expanding rapidly as they offer many advantages over conventional wireless links. They allow the use of very wideband radio links suitable for inter satellite and personal communications. Commercially available systems are under development at 28 GHz for the Local Multipoint Distribution System (LMDS) [1], the PCS networks at 38 GHz [2], [3], and also a new short range telecommunication band at 60 GHz. Commercial systems demand high yield and the ability to fabricate large volumes of systems using low cost techniques.

Current millimeter-wave wireless front-end transceivers use a hybrid approach with a combination of waveguide components, solid state devices, and dielectric resonators (Fig. 1). All of the active components (LNA, power amplifier, mixer) are based on solid state technology and are implemented using planar MMICs. However, the diplexer and other filters are implemented either using high Q structures such as resonant waveguide cavity filters or dielectric resonator filters. These expensive components are needed in order to have a low insertion loss, high out of band rejection, and high channel to channel isolation. The theoretical insertion loss of a filter is given by [4]:

$$\Delta L_A(dB) \approx 8.686 \frac{c_n}{\bar{\omega} Q_u} \tag{1}$$

where $\Delta L_A(dB)$ is the in band insertion loss, c_n is the filter prototype coefficient depending and is a function of the number of poles and passband ripple of the filter, $\bar{\omega}$ is the filter

This work is supported United States Army Research Office ASSERT under contract DAAH04-95-1-0205.

P. Blondy is with IRCOM, University of Limoges, Limoges, France. A. R. Brown and G. M. Rebeiz are with the Radiation Laboratory, Department of Electrical Engineering, University of Michigan, Ann Arbor, MI, 48109. E-mail: pblondy@ircom.unilim.fr, mscout@engin.umich.edu, rebeiz@engin.umich.edu

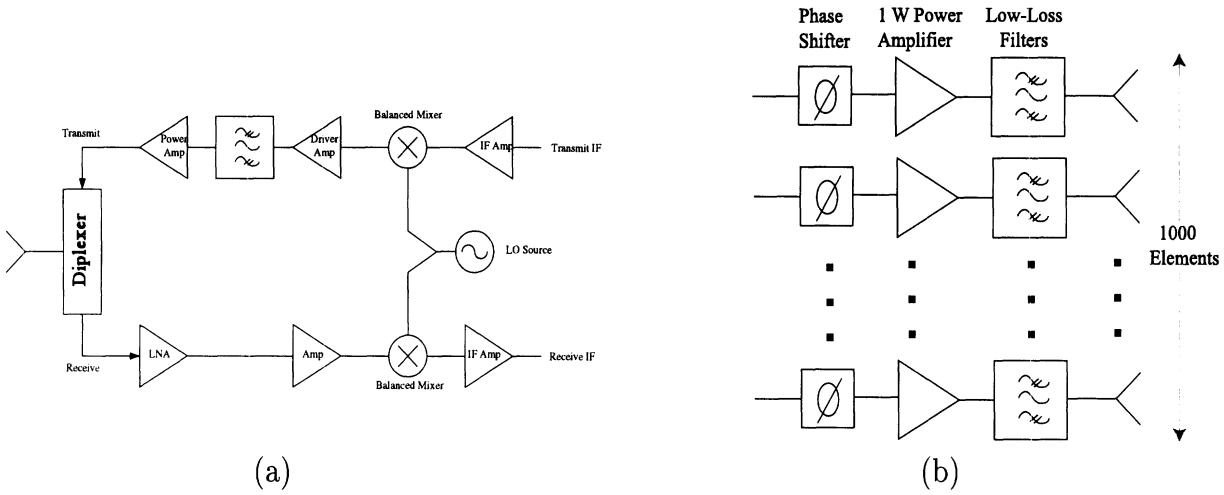

Fig. 1. Typical millimeter-wave (a) transceiver front-end block diagram and (b) new generation K-band phased array for satellite communications.

fractional bandwidth, and Q_u is the unloaded quality factor of the resonator. Figure 2 shows the impact of a the quality factor on the insertion loss of a 3% and an 8% filter. It is evident that in order to obtain high performance, a resonator unloaded Q of 500 or higher should be used for a narrow band diplexer design.

The local oscillator should also exhibit a very low-phase noise performance which is strongly dependent on the quality factor. The oscillator phase noise, using a linear approximation, is given by:

$$N_{pn}(f_m) = \frac{FkT}{2P_{avs}}\left[1 + \left(\frac{1}{2Q_L}\right)^2\left(\frac{f_0}{f_m}\right)^2\right] \tag{2}$$

where F is the noise figure of the active circuit with the positive feedback removed, k is the Boltzman constant, T is the temperature, P_{avs} is the available signal power, Q_L is the resonator loaded Q, f_0 is the oscillation frequency, and f_m is the frequency offset from the carrier where the noise spectral power is measured. For frequencies near the carrier, the phase noise is a function of $1/Q^2$. Millimeter-wave oscillators are typically fabricated with either a waveguide cavity such as the case of Gunn or IMPATT diodes [5] or using a dielectric resonator as in the case of HEMT or HBT devices [6], [7], [8]. These resonators exhibit a Q of 1000-3000 at 30-60 GHz and result in excellent phase noise performance. However, excellent performance is also achieved with a micromachined resonator with a Q of 500-1000.

This paper discusses alternative methods for obtaining *planar* high-Q elements by using micromachining techniques to alter the geometry of a silicon substrate. The paper presents two methods: the first technique is based on thin dielectric (membrane) technology and the second technique is based on three-dimensional etching in a cavity formation of a silicon wafer. The micromachined resonators are fully compatible with MMIC technology and most importantly, do not require low-loss millimeter-wave transitions which are necessary in waveguide technology. Also, micromachined resonators are lithographically defined and therefore do not require exact placement and manual tuning such as in dielectric resonator designs. It is expected that micromachining techniques will be very useful in future millimeter-wave communication and phased array systems.

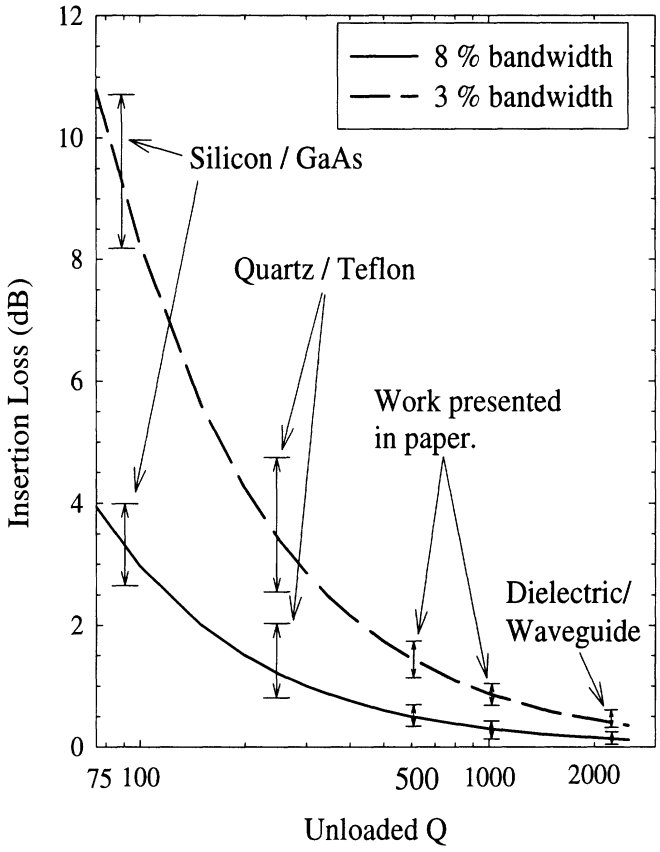

Fig. 2. Theoretical insertion loss for 3% and 8% filters. The estimated type of resonator is based on data from 30-60 GHz.

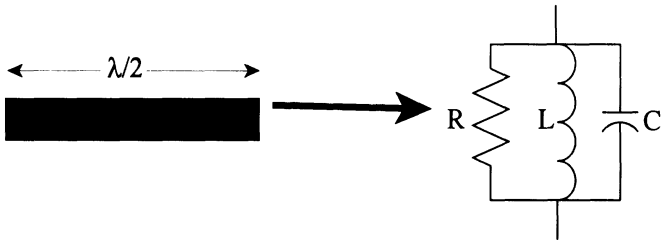

Fig. 3. Equivalent parallel RLC model for distributed resonator.

II. Definition of Quality Factor

The definition for the Q factor is given by:

$$Q = \omega \frac{\text{energy stored resonator}}{\text{energy dissipated}} \tag{3}$$

The equivalent circuit for a distributed resonator is taken as a parallel RLC lumped element model (Fig. 3). In order to excite the resonator, energy must be coupled into the resonator with either magnetic or electric coupling. To take into account the effects of input/output loading, the quality factor of a structure can be broken down into different figures of merit, namely the loaded Q (Q_L), the unloaded Q (Q_u), and the external Q (Q_{ext}). The loaded Q is the measured quality factor taking into account the loading effects of the resonator itself

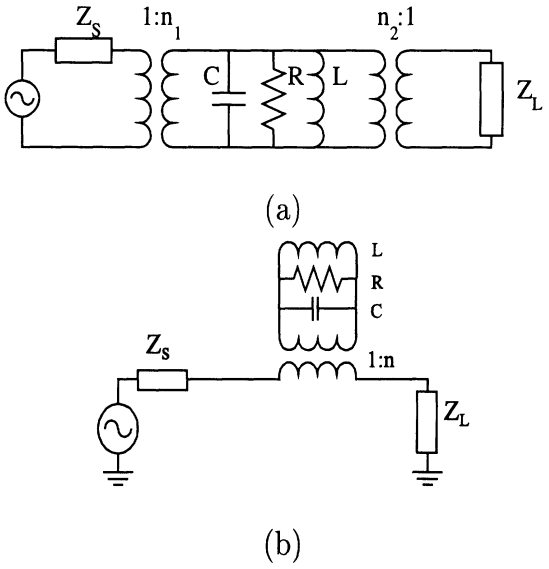

Fig. 4. Typical resonator configurations for magnetic coupling in (a) bandpass and (b) bandstop configuration

and also the loading of the external circuit. Only the loaded Q of a resonator can actually be measured, and the unloaded Q and the external Q of a resonator have to be extrapolated.

There are two main resonator configurations typically encountered in microwave and millimeter-wave circuits, namely the bandpass and the bandstop configurations. The bandpass configuration (fig. 4a) uses the resonator as a single resonator bandpass filter reflecting power at frequencies away from resonance and passing power at frequencies at resonance. The bandstop configuration (fig. 4b) allows power to pass by the resonator away from resonance, and then absorbs power from the line at resonance increasing the effective impedance and causing more reflection.

For a resonator in bandpass (bandstop) configuration with a resistive matched source and load impedance, the loaded quality factor can be obtained from measuring the 3 dB bandwidth of the S_{21} (S_{11}) as shown below:

$$Q_L = \frac{f_0}{\Delta f_{3dB}} \tag{4}$$

where f_0 is the resonant frequency and Δf_{3dB} is the 3 dB bandwidth of the S_{21} (S_{11}) response. The external Q can then be obtained from the loaded Q and the insertion loss of the resonator at the resonant frequency by solving:

$$Q_{ext} = \frac{Q_L}{S_{21}(f_0)} \quad \text{or} \quad \left(Q_{ext} = \frac{Q_L}{S_{11}(f_0)}\right) \tag{5}$$

where $S_{21}(f_0)$ (or $S_{11}(f_0)$) is the transmission (reflection) coefficient at resonance for the bandpass (bandstop) resonator and is measured in linear scale. The unloaded Q can be found from:

$$Q_u = \frac{Q_l}{1 - S_{21}(f_0)} \quad \text{or} \quad \left(Q_u = \frac{Q_l}{1 - S_{11}(f_0)}\right) \tag{6}$$

For accurate measurements, the coupling should be weak so that any influence of the loss of the feedline structure does not have a strong impact on the unloaded Q extrapolation.

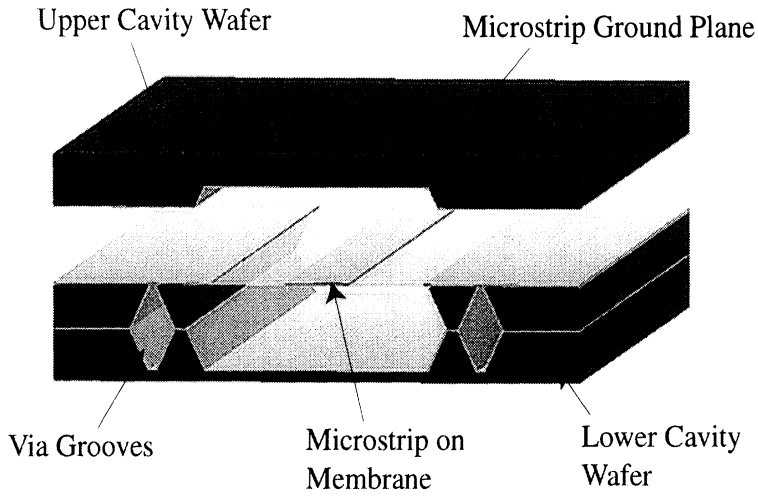

Fig. 5. Transverse section of the microstrip structure

The three definitions for the quality factor for both the bandpass and the bandstop configurations are given by:

$$\frac{1}{Q_u} = \frac{1}{Q_L} - \frac{1}{Q_{ext}} \tag{7}$$

III. Membrane Supported Suspended Microstrip Resonators

For the case of a distributed transmission line resonator, such as a microstrip or CPW resonator, the quality factor can be found by:

$$Q = \frac{\pi}{\lambda \alpha} \tag{8}$$

where λ is the guided wavelength and α is the attenuation in Np/m including attenuation by radiation, substrate loss, and ohmic loss. Distributed resonators using microstrip structures on conventional substrates have been used extensively for applications at X-band and below with reasonable values of Q (100-150 on quartz/Teflon). However, with increasing frequency, thinner substrates must be used to reduce radiation loss in substrate modes. This results in a narrow line dimensions for a given impedance which greatly increases the ohmic loss, and drastically reduces the resonator Q. Micromachining techniques are used to produce a micropackaged, air dielectric line with wide transverse dimensions resulting in high-Q resonators at millimeter-wave frequencies.

Membrane supported microstrip structures are formed by removing the silicon substrate and suspending a microstrip line on a thin (1.4 μm) dielectric membrane. A ground plane is formed by another micromachined substrate and attached to the top of the circuit. The bottom is also shielded with a third substrate (Fig. 5). For this structure, dielectric loss is eliminated with the air dielectric, the radiation loss is minimized by shielding the structure on all sides using thick via grooves to limit substrate modes, and ohmic loss is greatly reduced by allowing for very wide transverse microstrip geometries. Silicon has been used for its low cost anisotropic etching properties. Other materials can also be used such as InP and GaAs. In the past, micromachining techniques have been successfully applied to K and W-band membrane supported microstrip lines and filters [9], [10].

A. Fabrication

The micromachined suspended microstrip transmission line is based a three wafer process (Fig. 5). The top wafer will be referred to as the ground plane wafer, the middle wafer as the circuit wafer, and the bottom wafer as the shielding wafer. For the circuit wafer, a stress compensated 1.4 μm membrane layer consisting of $SiO_2/Si_3N_4/SiO_2$ (7000Å/4000Å/3000Å) is deposited on a high resistivity 525 μm thick silicon substrate using thermal oxidation and low pressure chemical vapor deposition. This process deposits the thin film on both sides of the silicon wafer allowing for a membrane on the top side of the wafer and a good etch mask for the silicon removal on the back side. The thicknesses of the SiO_2/Si_3N_4 layers are optimized to balance the net stress leaving the membrane in slight tension to result in flat and rigid membranes. After the membrane is deposited, the circuit is patterned on the top side of the wafer using either standard 2 μm gold electroplating technique or 1 μm evaporated gold and lift-off procedure depending on the operating frequency of the resonator. Other circuit components such as thin film capacitors, resistors, or air bridges can also be included at this time. Next, an opening is defined on the back side of the wafer under the resonators and areas where via holes are to be formed by etching the backside membrane with an RIE machine. The silicon is then completely etched under the circuit to the dielectric membrane which acts as an excellent etch stop. The etchant used in this work was a solution of 12.5% tetramethyl ammonium hydroxide (TMAH) and water [11]. This solution has a 1.1 μm/min etch rate for the $\langle 100 \rangle$ crystal plane with a $\langle 100 \rangle : \langle 111 \rangle$ selectivity of 25:1.

The bottom shielding wafer and the top ground plane wafer are 525 μm thick low resistivity wafers with a thermal oxide that acts as an etch mask. The bottom wafer is etched down 400 μm and metalized with gold to prevent radiation. The top ground plane wafer is formed by double side etching. First, a selective etch is performed on the upper side of the top wafer to begin probe window openings. Next, the lower side is patterned and the wafer is etched on both sides to open the probe windows and to form the upper cavity ground plane. The three wafers are finally assembled using conductive silver epoxy [12] to form the complete resonator.

B. Simulation and Measurement

Several resonators were constructed using both the bandpass and the bandstop configurations. In all cases, the resonators are $\lambda_0/2$ microstrip lines that are weakly coupled by capacitive coupling gaps or magnetically coupled by parallel coupled lines.

A single resonator was fabricated at 29 GHz in a bandstop configuration (Fig. 6). The ground plane height is 250 μm with an 800 μm wide conductor. The metal thickness of the conductor is 2 μm of electroplated gold (4 skin depths at 29 GHz). The shielding cavity is 800 μm away from the resonator. In order to conserve membrane space, the resonator was bent in a U shape using optimal miters. The length of the resonator was adjusted for the correct resonant frequency to 29.0 GHz by using a $2\frac{1}{2}$D moment method package IE3D [13]. The measured resonance was at 28.7 GHz showing a 1% shift in the resonant frequency. This is due to the fringing capacitance to the sidewalls of the cavity that was not modeled with the full wave analysis technique.

The suspended microstrip feedline is first measured without the resonator to study the effect of the CPW to microstrip transition. The microstrip line is 1025 μm wide resulting in an impedance of 50 Ω over a 250 μm ground plane. The transition can be modeled with a series inductor to account for the extra inductance between the CPW and microstrip ground planes. Figure 7 shows the measured and modeled S_{11}, and excellent agreement is achieved

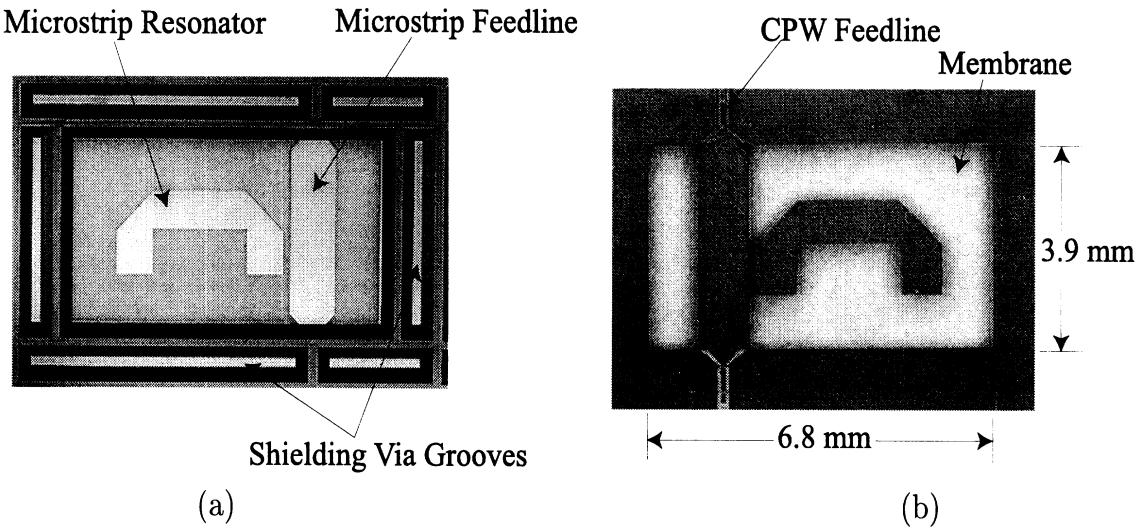

Fig. 6. Circuit wafer of a 29 GHz mircostrip resonator in bandstop configuration (a) bottom view and (b) top view.

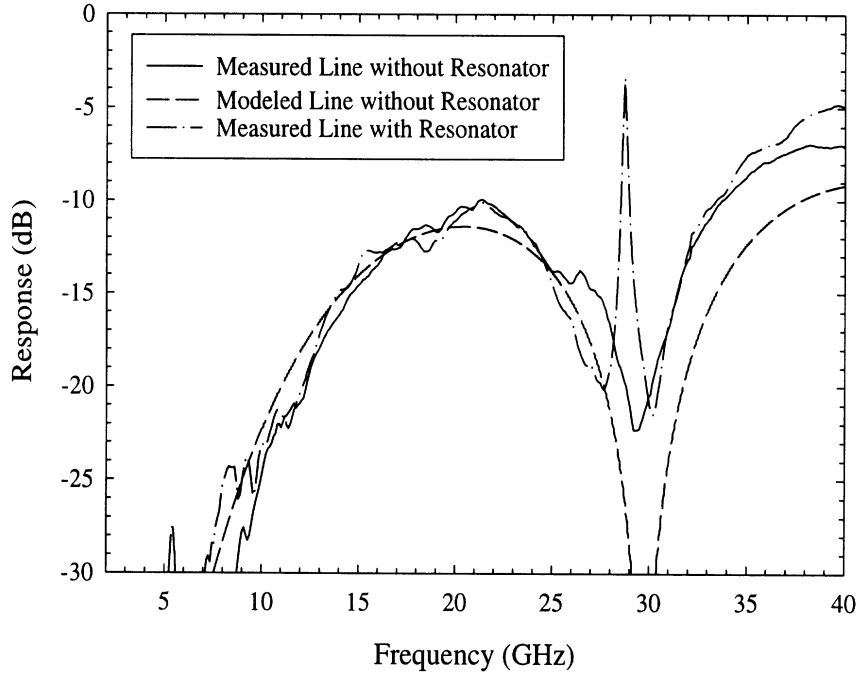

Fig. 7. Measured S_{11} of bandstop resonator including effects of transition.

with a 0.05 nH series inductance. Figure 7 also shows the S_{11} response with the resonator present. As shown, the microstrip line length is chosen to result in a good match at 27-32 GHz with the effects of the transition discontinuity. The measured loaded Q was 190 with a coupling -4.6 dB giving an extracted unloaded Q of 460 at 28.7 GHz.

Three different resonators were fabricated in bandpass configurations at 37 and 60 GHz. At 37 GHz, the resonator has a ground plane height of 200 μm and a line width and thickness of 700 μm and 2 μm, respectively. The extracted unloaded Q based on measurements is 412 at 37 GHz. Two different resonators were also fabricated at 60 GHz. Both resonators have a ground plane height of 250 μm with widths of 500 and 700 μm. The resonator thickness is 1 μm of evaporated gold (3 skin depths at 60 GHz). The 500 μm lines had an extracted

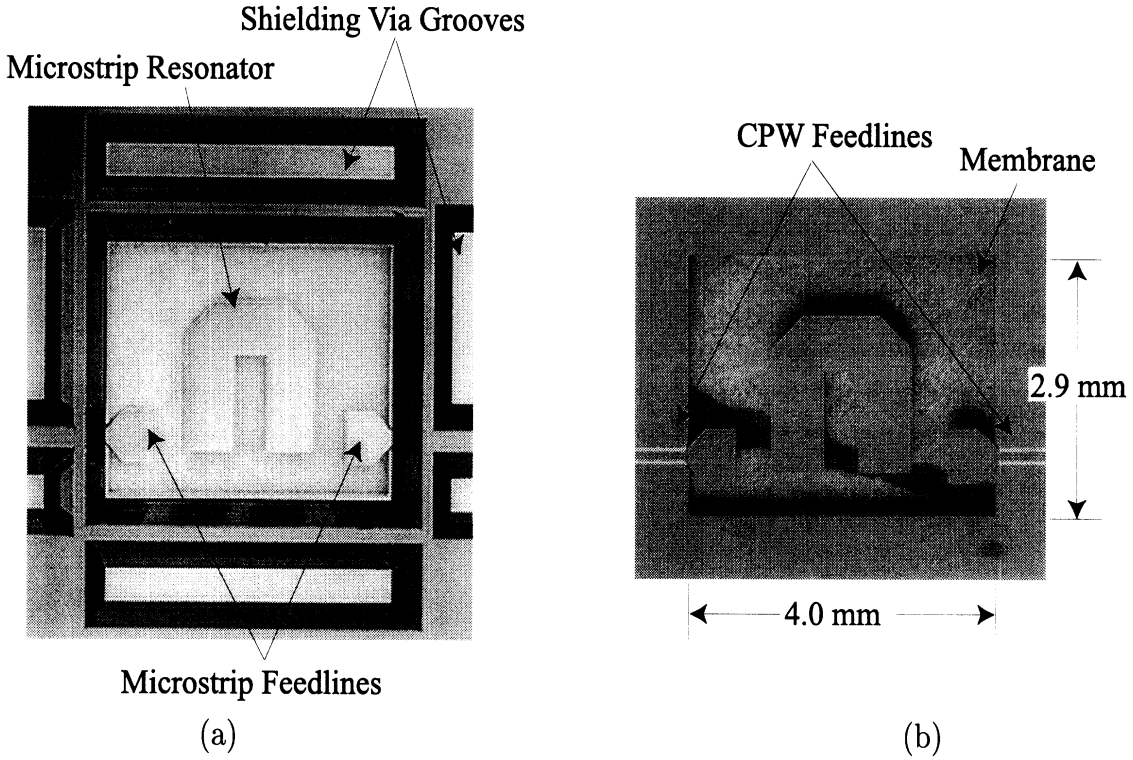

Fig. 8. Bandpass configuration of 37 GHz micromachined microstrip resonator (a) bottom view and (b) top view.

unloaded Q of 454 and the 700 μm lines had an extracted unloaded Q of 503. Some of these resonators have been used in state-of-the-art low loss filters at 37 and 60 GHz [14].

The four structures described above were simulated using method of moments based HP-Momentum [15], a finite element tool [16], an empirical model from Linecalc [17], and a code based on the surface impedance method called Simian [18]. For the simulations, the conductivity of the gold lines was assumed to be $3.9 \times 10^7\ \Omega^{-1}m^{-1}$. The results for the simulations and measurements are summarized in Table I. The values based on Linecalc, MoM, and FEM all overestimate the value for the unloaded Q considerably. However, Simian models the loss very accurately and is within 5% of the measured values. The measured Q_u values are 10$\times$ larger than microstrip resonators on GaAs or Silicon, and 2$\times$ larger than corresponding resonators on low dielectric constant substrates such as Teflon.

Design curves for the Q factor were generated using Simian (Fig. 9) for both the 30 GHz (t=2 μm gold) and 60 GHz (t=2 μm gold) resonators. For the 60 GHz calculations, increasing the metal thickness to 2 μm will result in a 2-3% improvement in Q. The value of the resonator Q is very sensitive to the ground plane height. However, with increasing height (h> 250 μm), the CPW to membrane transition becomes more difficult with added transition inductance from the CPW ground to the microstrip ground plane. Also, increasing the width of the lines past 800-900 μm resulting in very wide transmission lines and makes circuit modeling and design more difficult. Therefore, practical considerations will limit the Q of such resonators to 450-550 for most applications.

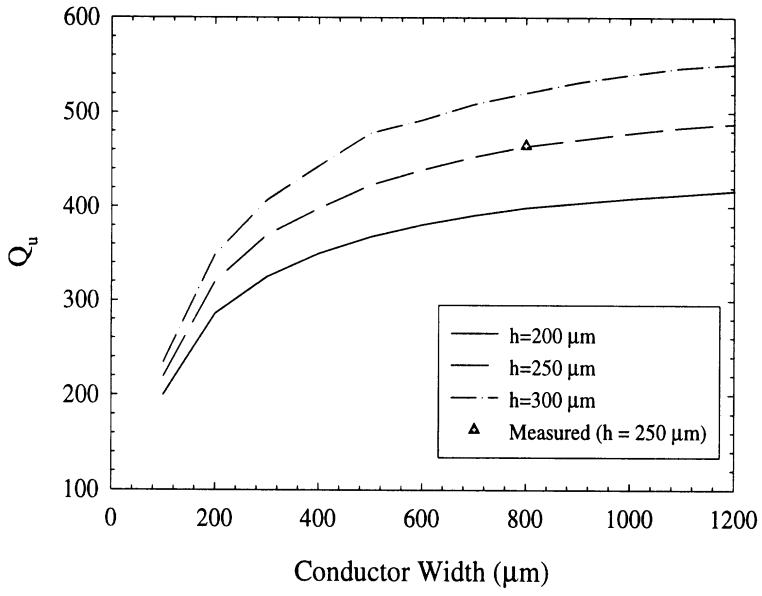

(a)

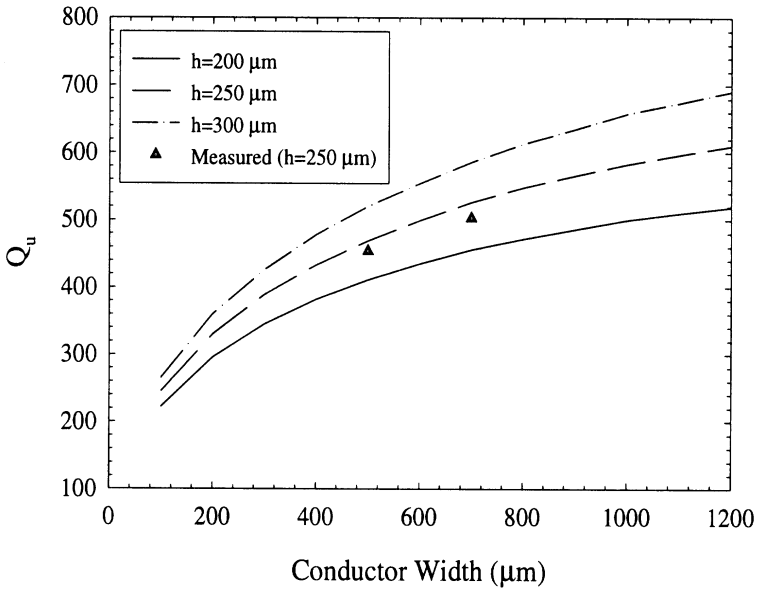

(b)

Fig. 9. Simulated (Simian) microstrip resonator Q as a function of height and strip width at (a) 30 GHz with 2 μm thick lines and (b) 60 GHz 1 μm thick lines.

IV. Integrated Micromachined Cavity Resonators

The quality factor of the suspended microstrip line shows a large improvement over conventional microstrip lines, but in many cases, an unloaded quality factor of 500 is still not enough. One way to increase the resonator Q is to integrate miniature 3-dimensional cavities in the silicon substrate.

The integrated micromachined waveguide resonator was first demonstrated at 10 GHz for the case of very strong transmission coupling using a two wafer process with a slot-aperture coupling [19]. The slot was excited by a microstrip line above it. This method requires two wafers: one for the microstrip to slot transition, and the second for the actual cavity

TABLE I
COMPARISON BETWEEN MEASURED AND SIMULATED VALUES OF UNLOADED Q.

Q_u	w=800 μm h=250 μm fo=29 GHz	w=700 μm h=200 μm fo=37 GHz	w=700 μm h=250 μm fo=62 GHz	w=500 μm h=250 μm fo=62 GHz
linecalc [17]	528	474	665	606
FEM [16]		442	661	610
MoM [15]	550	470	613	536
Simian [18]	450	403	525	474
Measured	460	412	503	454

(Fig. 10a). However, the Q of the resonator is strongly related to the thickness of the cavity, which, in this case, is limited to a standard thickness wafer. Also, at millimeter-wave frequencies, the microstrip line must be integrated on a thin substrate (250 μm at 30 GHz, 150 μm at 60 GHz, etc.) with the expected additional circuit losses.

A new approach is presented for feeding the cavity that increases the quality factor and simplifies the fabrication. The cavity is constructed from two standard thickness (525 μm) silicon wafers etched 450 μm down. A CPW line is defined on the bottom wafer to the edge of the cavity, and a wire bond is placed from the end of the CPW line to the base of the cavity. This acts as an electric loop triggering the dominant TE_{011} mode at resonance. The amount of coupling is controlled by the length of the wire bond and the number of bonds placed. The top cavity is identical to the bottom cavity except a groove (called a "mouse hole") is etched above the CPW line on the bottom cavity. The groove is to prevent shorting the CPW line when the two wafers are bonded together (Fig. 10b). The two wafers are bonded together with conductive epoxy. For minimal cavity disturbance, the feedlines and wire bonds are placed where the current on the side walls of the cavity are at a minimum. For the case of a rectangular cavity, the corners have a current null. Using this method, the maximum operating frequency is set by the dimensions of the CPW feedlines and not the substrate thickness, and the Q is increased by increasing the cavity height by a factor of two using standard thickness substrates.

A. Fabrication

A thermal oxide is grown on two standard thickness silicon wafers to act as an etch mask for the micromachining process. The bottom wafer that contains the feedlines is a high resistivity substrate (2000 Ω-cm) and the top wafer is a low resistivity substrate (5-7 Ω-cm). The CPW feedlines are deposited on the bottom wafer using a gold electroplating process. Next, the oxide where the cavity is to be etched is removed with a wet chemical etch. The cavity resonator is defined 500 μm away from the end of the CPW feedline. The designed cavity dimensions are 8.84 mm $\times$ 8.84 mm for a TE_{011} resonant frequency of 24 GHz. The cavity is then etched 450 μm in an anisotropic silicon etchant (TMAH). The etchant has a selectivity to the $\langle 100 \rangle : \langle 111 \rangle$ crystal plane of approximately 25:1. This gives an undercut of roughly 15 μm leaving a small SiO_2 lip. It is essential to remove this lip in BHF to eliminate any gold shadowing due to the lip and thus result in a very low Q. The CPW feedlines are then masked with photoresist and the entire cavity is metalized with a 3 μm layer of sputtered and electroplated gold. Four 18 μm thick gold wirebonds in parallel are used to

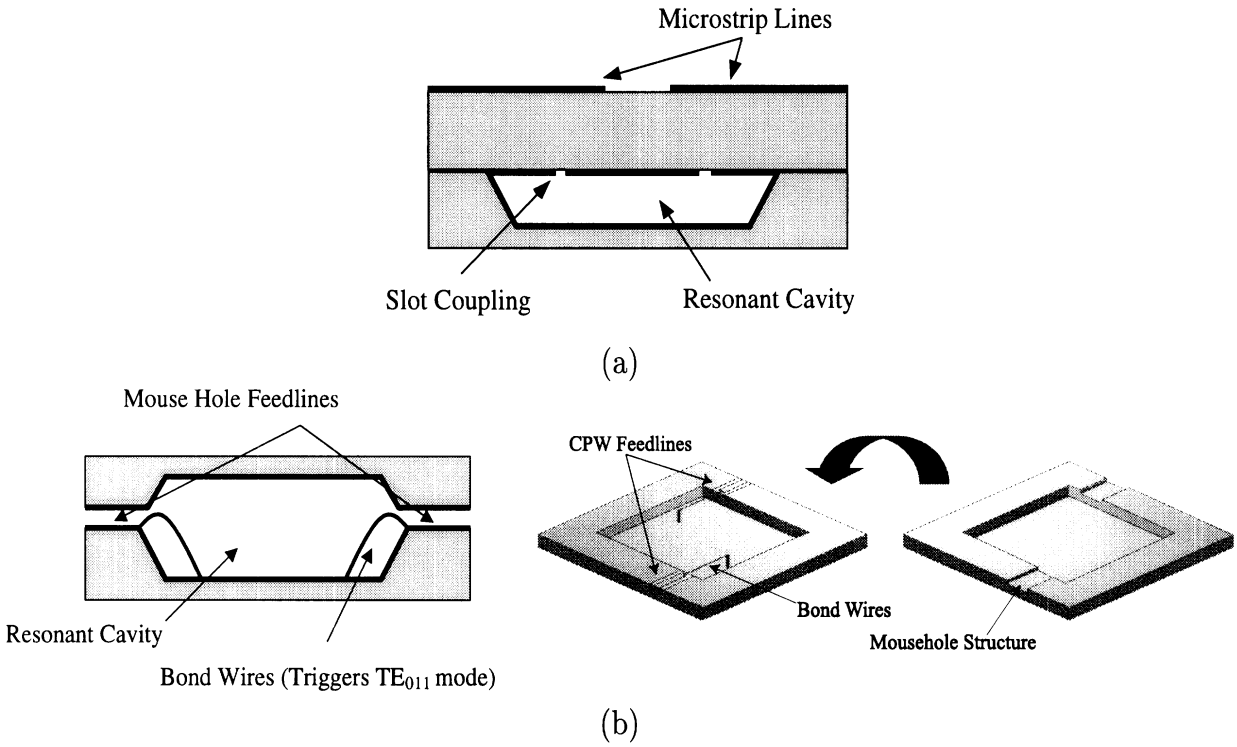

Fig. 10. Side view of micromachined cavity resonator (a) method used by Papapol, et al. and (b) method used in this work.

excite the cavity. The wirebonds were approximately 1.2 mm long placed from the feedline in the corner of the cavity diagonally toward the center of the cavity with a calculated series inductance of 0.5 nH.

The top wafer is fabricated using a two step etch to allow for the "mouse holes" above the CPW feedlines. First, the cavity and the feedline mouse holes are patterned and the oxide is etched half way through. Next, the cavity alone is patterned and the remaining oxide covering the cavity is etched exposing the bare silicon. The substrate is then placed in the anisotropic etchant and the cavity is etched 350 μm down. The remaining oxide covering the feedline mouseholes is carefully etched away making sure not to completely etch the oxide protecting the surrounding areas. Again, the substrate is placed in the silicon etchant for another 100 μm of etching yielding a cavity depth of 450 μm and the mousehole depth of 100 μm. The thermal oxide is completely stripped off eliminating the lip formed from the undercut of the silicon etching. The top wafer is then metalized with a 3 μm layer of sputtered and electroplated gold. The two substrates are bonded using conductive epoxy.

B. Simulation

The unloaded quality factor of a resonant cavity is found from [20]:

$$Q_u = \omega \frac{W_m + W_e}{P_l} \tag{9}$$

where W_m and W_e are the energies stored in the magnetic and electric fields respectively, and P_l is the net power dissipated. In the case of the air filled cavity, the net power dissipated is purely the ohmic loss from the currents on the sides of the resonator. By neglecting the effects of the non-vertical sidewalls, the effects of the mousehole, any imperfections in bonding, and the by assuming all the current is concentrated in one skin depth, the quality

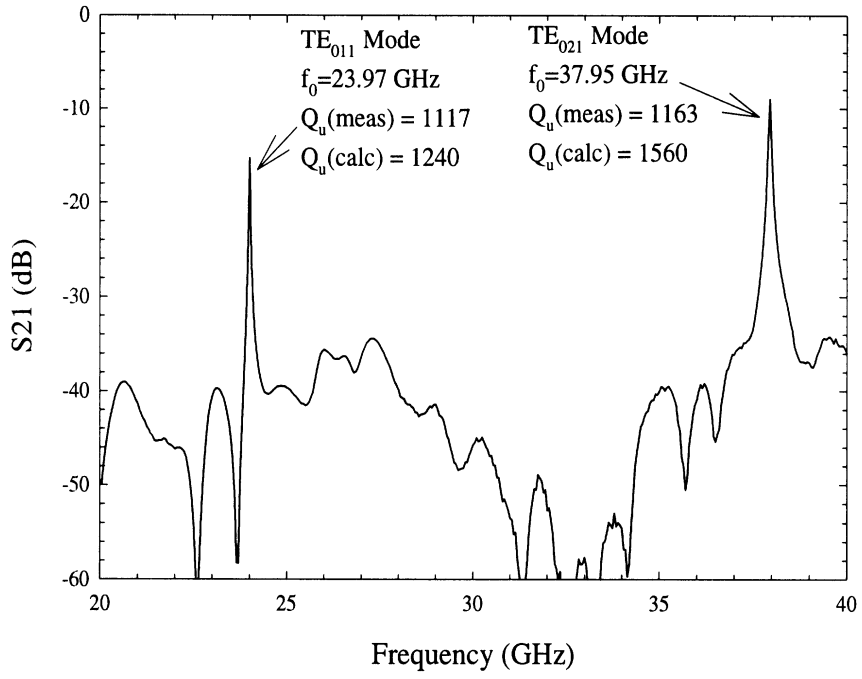

Fig. 11. Two wafer micromachined cavity resonator.

factors for different resonances can be easily calculated using the known current and field distribution for a given cavity mode. The unloaded quality factor for the first two modes are 1240 for the TE_{011} at 24 GHz and 1560 for the TE_{021} mode at 38 GHz using the conductivity of gold as $3.9 \times 10^7\ \Omega^{-1}m^{-1}$.

C. Measurements

The cavity resonator was measured with an HP8510C using an SOLT calibration with the probe tips as the calibrated reference plane. The measured TE_{011} resonant mode was 23.97 GHz which is in excellent agreement with the designed value of 24 GHz. At resonance, the measured S_{21} is -15.2 dB with a loaded quality factor (Q_l) of 909, resulting in an Q_u of 1100, which is in good agreement with the calculated value of 1237. The calculated value does not include the increase resistance from the silver epoxy bonding, the effects of the mouse holes altering the current distribution on the resonator, or the loss in the 2 mm CPW feedlines. The combined loss of both feedlines is 0.6 dB. Subtracting this from the measured S_{21} gives a Q_u of 1117. The TE_{021} occurs at 37.95 GHz with a measured value of Q_l of 690 with an S_{21} of -7.9 dB. When the loss of the CPW feedlines (0.75 dB at 38 GHz) is removed, Q_u is 1163. To the author's knowledge, this is the highest Q integrated resonator to date at K-band, and could be used in low-phase noise millimeter-wave oscillator designs.

V. Conclusions

Micromachining techniques have been applied to fabricate high-Q integrated resonators. The fabrication is compatible with most CMOS and MMIC processes. Micromachined suspended microstrip lines exhibit quality factors in the range of 450-500 at 29, 37, and 62 GHz in both bandpass and bandstop configurations. Furthermore, calculations using Simian show that practical considerations limit the Q of suspended microstrip resonators to 550.

These resonators can be easily used in complex filter designs [14]. Integrated miniature waveguide cavity resonators have also been fabricated at 24 GHz (dominant mode) with a quality factor of 1100-1200. The micromachined waveguide cavities can be readily scaled to 60 GHz (3.5 mm $\times$ 3.5 mm $\times$ 800 μm with a calculated $Q_u = 1600$) and to 77 GHz (2.8 mm $\times$ 2.8 mm $\times$ 800 μm with a calculated $Q_u = 1670$) using standard thickness wafers for communication systems and automotive radars.

VI. Acknowledgements

This work was supported by the U.S. Army Research Office ASSERT under contract DAAH04-95-1-0205. The authors would like to thank Dr. G. Ponchak, NASA-Lewis Research Center, for providing the 60 GHz measurement setup.

References

[1] Douglas A. Gray, "A Broadband Wireless Access System at 28 GHz," *1997 Wireless Communications Conference Proceeding*, pp. 1–7, 1997.

[2] Holger H. Meinel, "Commercial Applications of Millimeter-waves. History, Present Status and Future Trends," *IEEE Transactions on Microwave Theory and Techniques*, vol. 43, no. 7, pp. 1639–1653, July 1995.

[3] John Burns, "The Application of Millimetre-wave Technology for Personal Communication Networks in the United Kingdom and Europe: a Technical and Regulatory Overview," *IEEE MTT-S Internation Microwave Symposium Digest*, pp. 635–638, 1994.

[4] G. L. Matthaei, L. Young, and E. M. T. Jones, *Microwave Filters, Impedance-Matching Networkds, and Coupling Structures*, Artech House, 1980.

[5] Shigemichi Nagano and Shuji Ohnaka, "A Low-Noise 80 GHz Silicon IMPATT Oscillator Highly Stabilized with a Transmission Cavity," *IEEE Transactions on Microwave Theory and Techniques*, vol. 22, no. 12, pp. 1152–1159, Dec. 1974.

[6] M. Funabashi, T. Inoue, K. Ohata, K. Maruhashi, K. Hosoya, M. Kuzuhara, K. Kanekawa, and Y. Kobayashi, "A 60 GHz MMIC Stabilized Frequency Source Composed of a 30 GHz DRO and a Doubler," *IEEE MTT-S Internation Microwave Symposium Digest*, pp. 71–74, 1995.

[7] S. Chen, S. Tadayon, T. Ho, K. Pande, P. Rice, J. Adair, and M. Ghahremani, "U-Band MMIC HBT DRO," *IEEE Microwave and Guided Wave Letters*, vol. 4, no. 2, pp. 50–52, Feb. 1994.

[8] H. Wang, K. Chang, L. Tran, J. Cowles, T. Block, E. Lin, G. Dow, A. Oki, D. C. Streit, and B. Allen, "Low Phase Noise Millimeter wave Frequency Sources Using InP-based HBT MMIC Technology," *IEEE Journal of Solid-State Circuits*, vol. 31, no. 10, pp. 1419–1425, Oct. 1996.

[9] Gabriel M. Rebeiz, Linda P. B. Katehi, Thomas M. Weller, Chen-Yu Chi, and Stephen V. Robertson, "Micromachined Membrane Filters for Microwave and Millimeter-Wave Applications," *International Journal of Microwave and Millimeter-Wave CAE*, , no. 7, pp. 149–166, 1997.

[10] Chen-Yu Chi and Gabriel M. Rebeiz, "Conductor-Loss Limited Stripline Resonator and Filters," *IEEE Transactions on Microwave Theory and Techniques*, vol. 44, no. 4, pp. 626–630, Apr. 1996.

[11] Osamu Tabata, Ryouji Asahi, Hirofumi Funabashi, Keiichi Shimaoka, and Susumu Sugiyama, "Anisotropic Etching of Silicon in TMAH Solutions," *Sensors and Actuators A*, , no. 34, pp. 51–57, 1992.

[12] Epotek H20E, ," Epoxy Technology, 14 Fortune Drive, Billerica, MA.

[13] *Zeland IE3D, Release 4.12*, 1997.

[14] Pierre Blondy, Andrew R. Brown, Dominique Cros, and Gabriel M. Rebeiz, "Low Loss Micromachined Filters for Millimeter-Wave Telecommunication Systems," *IEEE MTT-S Internation Microwave Symposium Digest*, pp. 1181–1184, 1998.

[15] *Hewlett Packard Momentum, Release 2.0*, 1997.

[16] M. Aubourg and P. Guillon, "A mixed finite element formulation for microwave devices problems. Application to MIS structure," *Journal of Electromagnetic Waves and Applications*, vol. 5, no. 45, pp. 371–386, 1991.

[17] *Hewlett Packard Linecalc*, 1997.

[18] Sangwoo Kim, E. Tuncer, B-T Lee, and Dean P. Neikirk, *Surface Impedance Method for Interconnect Analysis*, http://weewave.mer.utexas.edu/MedHome.html, 1997.

[19] John Papapolymerou, Jui-Ching Cheng, Jack East, and Linda P. B. Katehi, "A Micromachined High-Q X-Band Resonator," *IEEE Microwave and Guided Wave Letters*, vol. 7, no. 6, pp. 168–170, June 1997.

[20] Robert E. Collin, *Foundations for Microwave Engineering*, McGraw-Hill, Inc., New York, 1992.